

## Raman scattering from acoustic phonons confined in Si nanocrystals

Minoru Fujii and Yoshihiko Kanzawa

*Division of Science of Materials, The Graduate School of Science and Technology, Kobe University, Rokkodai, Nada, Kobe 657, Japan*

Shinji Hayashi and Keiichi Yamamoto

*Department of Electrical and Electronics Engineering, Faculty of Engineering, Kobe University, Rokkodai, Nada, Kobe 657, Japan*

(Received 3 June 1996)

We have observed Raman scattering from acoustic phonons confined in Si nanocrystals. It was found that the Raman spectra depend strongly on the size of the nanocrystals and the peaks shift to higher frequencies as the size decreases. We also found that the depolarized Raman spectra appear at much lower frequencies than the polarized ones. [S0163-1829(96)50136-0]

Since the discovery of the highly efficient photoluminescence from porous Si,<sup>1</sup> optical properties of various types of Si nanostructures have been intensively studied.<sup>2-4</sup> Because of the small size of these systems, their distinct optical properties are considered to stem from three-dimensional confinement of electrons and holes as well as phonons. Until now, the effects of confinement on optical phonons in Si nanostructures have been widely studied by Raman spectroscopy and size-dependent shifts and broadening of the TO peak have been commonly observed.<sup>5-9</sup> In contrast to many studies for the optical phonons, to our knowledge, acoustic phonons confined in Si nanostructures have not been studied so far. Information on the confined acoustic phonons is indispensable for the discussion of electron-phonon interactions in Si nanostructures.<sup>10</sup>

The purpose of this work is to experimentally observe the acoustic phonons confined in Si nanocrystals and reveal the size dependencies. Until now, Raman scattering from confined acoustic phonons has been reported for some metal<sup>11-13</sup> and semiconductor nanocrystals.<sup>14-16</sup> However, observation of those in Si nanocrystals has not been successful, due mainly to the difficulties in preparing nanometer-size Si crystals. Recently, we have succeeded in preparing Si nanocrystals with good crystallinity as small as 3–5 nm in diameter dispersed in SiO<sub>2</sub> thin films. For these nanocrystalline Si samples, we could clearly observe the Raman spectra attributable to the acoustic phonons confined in Si nanocrystals. We will demonstrate that the spectra strongly depend on the particle size and the peaks shift to higher frequencies as the size decreases.

Samples were prepared by an rf cosputtering method similar to those used in our previous work.<sup>12,17</sup> Small pieces of Si tips 5×15×0.5 mm<sup>3</sup> in size were placed on a SiO<sub>2</sub> target (4 in. in diameter) and they were cosputtered. After the deposition, the samples were annealed in a N<sub>2</sub> ambient for 30 min at 1100 °C. The size of Si nanocrystals were controlled by changing the number of Si tips during the cosputtering. Throughout this work, the sizes of Si nanocrystals were determined from high-resolution electron microscopic (HREM) observations. The samples for the cross-sectional HREM observations were prepared by standard procedures including mechanical and Ar-ion thinning techniques. HREM observations were made using a JEM-200CX (JEOL)

electron microscope. Raman measurements were carried out in a back-scattering configuration at room temperature using a Jobin Yvon U1000 double monochromator and photon-counting system. The excitation source was the 488-nm line of an Ar-ion laser. To investigate polarization properties, we observed polarized and depolarized scattering spectra by setting the excitation and detection polarizations either parallel or perpendicular to each other.

Figure 1 shows a typical electron micrograph of Si nanocrystals embedded in a SiO<sub>2</sub> matrix. We can clearly see lattice fringes corresponding to the {111} planes of Si nanocrystals. It is found that each Si nanocrystal is a single crystal with good crystallinity and they are well dispersed in SiO<sub>2</sub> matrices. The average size of Si nanocrystals obtained from this micrograph was 5.5 nm.

Figures 2(a) and 2(b) show the size dependencies of the polarized and depolarized Raman spectra, respectively. In Fig. 2(a), a Raman peak can clearly be seen in each spectrum. The sample with diameter (*d*) of 5.5 nm exhibits a peak at 20 cm<sup>-1</sup>. As the size decreases, the peak shifts to higher frequencies and reaches 32 cm<sup>-1</sup> for *d*=3.1 nm. In

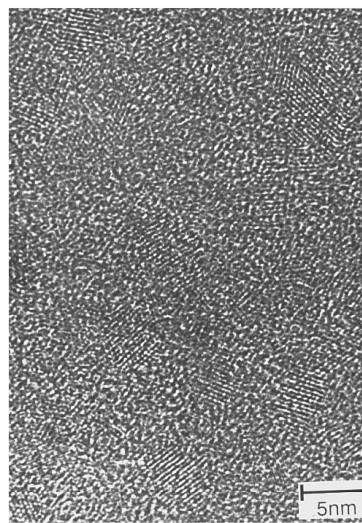


FIG. 1. Typical HREM image of Si nanocrystals embedded in a SiO<sub>2</sub> matrix. Lattice fringes corresponding to the {111} planes of Si can clearly be seen.

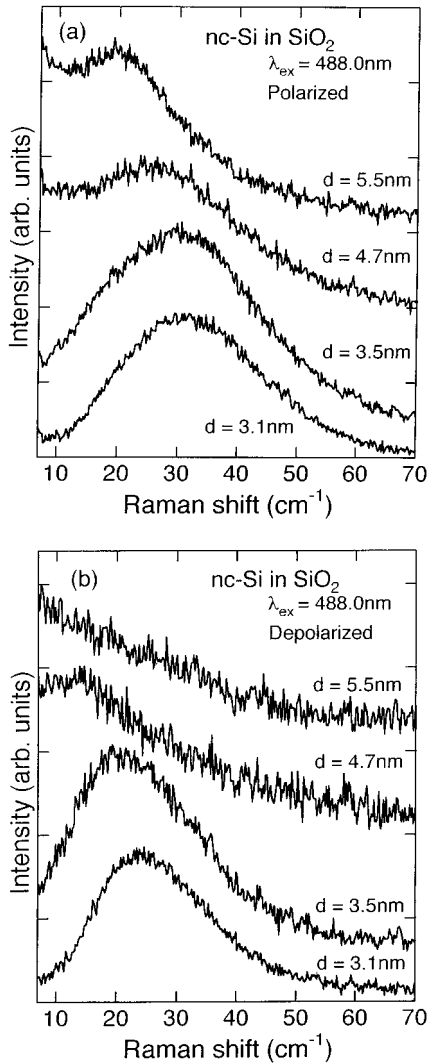


FIG. 2. Size dependence of (a) polarized and (b) depolarized Raman spectra of Si nanocrystals embedded in  $\text{SiO}_2$  matrices.

depolarized spectra [Fig. 2(b)], similar high-frequency shift of the peak with decreasing the size is observed. However, peak frequencies of the depolarized spectra are much lower than those of polarized spectra. Furthermore, we cannot observe a distinct peak for  $d = 5.5$  nm in the depolarized spectra. The intensity ratio of peaks in the polarized and depolarized spectra were about 0.25 for samples with  $d = 3.1$  and 3.5 nm. In order to see more clearly the size dependencies of the peak frequencies, we plot the peak frequencies as a function of inverse diameter in Fig. 3. The solid lines are the results of the least squares fitting by straight lines. Other lines are calculated results explained later. In Fig. 3, we can see that the peak frequencies ( $\omega_{\text{max}}$ ) depend strongly on the diameter ( $d$ ) and are inversely proportional to  $d$  within the accuracy of the experiment.

The observed  $\omega_{\text{max}} \propto d^{-1}$  relations of the low-frequency Raman spectra have also been reported for Ag,<sup>12</sup> Au,<sup>13</sup> and CdS (Ref. 16) nanocrystals. Furthermore, the characteristic polarization properties observed are very similar to those observed for Ge (Ref. 18) and CdS (Ref. 16) nanocrystals embedded in  $\text{GeO}_2$  matrices. In these previous work, observed peaks were attributed to the acoustic phonons confined in

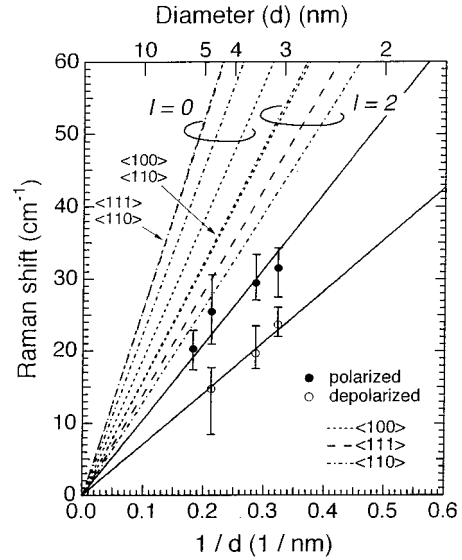


FIG. 3. Peak frequencies of polarized (filled circles) and depolarized (open circles) Raman spectra as a function of the inverse particle diameter. Solid lines are the results of the least squares fitting. Dotted, broken, and dashed-dotted lines are the results of theoretical calculations for the confined acoustic modes (spheroidal modes with  $l=0$  and 2) assuming the sound velocities in  $\langle 100 \rangle$ ,  $\langle 111 \rangle$ , and  $\langle 110 \rangle$  directions, respectively.

nanocrystals, because the peak frequencies agreed very well with the calculated eigenfrequencies of the confined acoustic phonons. The similarities of the size and polarization dependencies of the present Raman spectra with those of other nanocrystalline samples allow us to conclude that the presently observed low-frequency spectra are due to acoustic phonons confined in Si nanocrystals. To our knowledge, this is the first report on the observation of the confined acoustic phonons in Si nanocrystals.

The confined acoustic phonons in an elastic sphere were first theoretically studied by Lamb.<sup>19</sup> Two types of confined acoustic modes, spheroidal and torsional modes, were derived. The frequencies of these two modes are proportional to the sound velocities in particles and inversely proportional to the particle size. The spheroidal mode is characterized by the quantum number  $l \geq 0$ , while the torsional modes are characterized by  $l \geq 1$ . From the symmetry arguments, Raman-active modes are spheroidal modes with  $l=0$  and 2.<sup>20</sup> The  $l=0$  mode is purely radial with spherical symmetry and produces totally polarized spectra, while the  $l=2$  mode is quadrupolar and produces partially depolarized spectra. The depolarization factor is estimated to be  $\frac{1}{3}$  for spherical particles.<sup>21</sup>

We now calculate the eigenfrequencies of the confined acoustic modes assuming an elastic sphere with a free surface based on the theory developed by Lamb.<sup>19,22</sup> Although this model extremely simplifies the actual Si nanocrystals, this has been employed in many previous works and could explain experimental results very well.<sup>11–16,23</sup> The calculation needs longitudinal and transverse sound velocities and a mass density of nanocrystals. Since Si is elastically asymmetric, we made calculations using sound velocities corresponding to sound waves propagating in  $\langle 100 \rangle$ ,  $\langle 111 \rangle$ , and

TABLE I. Sound velocities of Si and calculated nondimensionalized eigenfrequencies ( $\eta = \omega d / 2v_l$ , where  $\omega$  is the angular frequency and  $d$  is the particle diameter). Sound velocities for three different directions were derived from elastic constants  $c_{11} = 16.57$ ,  $c_{12} = 6.39$ , and  $c_{44} = 7.956 \times 10^{10}$  N/m<sup>2</sup>, and mass density  $\rho = 2332$  kg/m<sup>3</sup> (Ref. 24).

Direction	$v_l$ (m/sec)	$v_t$ (m/sec)	$\eta(l=0)$	$\eta(l=2)$
$\langle 100 \rangle$	8429	5841	3.1	2.6
$\langle 111 \rangle$	9351	5092	4.9	2.6
$\langle 110 \rangle$	9129	4672	5.3	2.6
		5841	3.7	2.6

$\langle 110 \rangle$  directions. Sound velocities were derived from elastic constants  $c_{11} = 16.57$ ,  $c_{12} = 6.39$ , and  $c_{44} = 7.96 \times 10^{10}$  N/m<sup>2</sup>, and a mass density  $\rho = 2332$  kg/m<sup>3</sup>.<sup>24</sup> Four sets of sound velocities used for the calculations are listed in Table I. Note that TA phonon branches in  $\langle 100 \rangle$  and  $\langle 111 \rangle$  directions are twofold degenerate, while those in  $\langle 110 \rangle$  direction are not degenerate. The calculated nondimensionalized eigenfrequencies for spheroidal modes with  $l=0$  and 2 are also listed in Table I.

The dotted, broken, and dashed-dotted lines in Fig. 3 represent the Raman peak frequencies of the spheroidal modes with  $l=0$  and 2 calculated using the sound velocities in  $\langle 100 \rangle$ ,  $\langle 111 \rangle$ , and  $\langle 110 \rangle$  directions, respectively. Due to the anisotropy of the elastic constants, the calculated frequencies are scattered depending on the direction. In Fig. 3, we can see that, even if we take into account the anisotropy, the agreement between experiments and calculations are very poor. The calculated frequencies are much larger than those of the observed peaks for both the polarized and depolarized spectra. This suggests that the assumption of free elastic sphere is not valid in the present Si nanocrystals.

The Si nanocrystals in the present work are dispersed in SiO<sub>2</sub> matrices. The SiO<sub>2</sub> matrices may cause the low-frequency shifts of the confined acoustic modes. The effects of surrounding matrices on the confined acoustic modes have recently been discussed by several authors.<sup>18,21,22</sup> They

showed that the surface modes (the lowest frequency mode for each  $l$ ) are softened and broadened, if Lamé's constants  $\lambda$  and  $\mu$  and the mass density  $\rho$  of matrices approach those of nanocrystals. However, quantitative estimations of the shift and broadening are still lacking. In particular, completely opposite predictions were recently made for the influences of SiO<sub>2</sub> matrices on the Ag particles. Montagna and Dusi<sup>21</sup> showed that the influences are very small and negligible, while Ovsyuk and Novikov<sup>18</sup> reported that the matrix effects are non-negligible and the surface modes shift to lower frequencies by considerable amounts. Further theoretical studies are required to quantitatively discuss the matrix effects.

In the above discussion, we assumed that the nanocrystal is a homogeneous elastic body. This assumption is valid provided that the nanocrystal is large enough and does not have large anisotropy in the elastic constants. The small size limit of the applicability of the continuum assumption has not yet been examined theoretically. In the present nanocrystals, the continuum assumption may not be applicable and a more rigorous calculations may be necessary. It seems to be very interesting to compare the present results with those obtained by the lattice dynamical calculations.

In summary, we have succeeded in observing Raman scattering from acoustic phonons confined in Si nanocrystals. We could experimentally determine the size dependencies of the frequencies of the confined acoustic phonons. The present data are considered to be very useful in estimating the size of other types of Si nanostructures such as those in porous Si by Raman spectroscopy. However, due to the large anisotropy of the elastic constants and the matrix effects, quantitative comparison between experiments and theory were not successful. Further experimental and theoretical studies are required in fully understanding the size dependencies of the confined acoustic phonons.

We are indebted to Professor A. Tamura of Saitama Institute of Technology for valuable discussions and suggestions. This work was partially supported by a grant from Foundation Advanced Technology Institute.

<sup>1</sup>L. T. Canham, Appl. Phys. Lett. **57**, 1046 (1990).

<sup>2</sup>H. Takagi, H. Ogawa, Y. Yamazaki, A. Ishizaki, and T. Nakagiri, Appl. Phys. Lett. **56**, 2379 (1990).

<sup>3</sup>H. Morisaki, F. W. Ping, H. Ono, and K. Yazawa, J. Appl. Phys. **70**, 1869 (1991).

<sup>4</sup>K. A. Littau, P. J. Szajowski, A. J. Muller, A. R. Kortan, and L. E. Brus, J. Phys. Chem. **97**, 1224 (1993).

<sup>5</sup>H. Richter, Z. P. Wang, and L. Ley, Solid State Commun. **39**, 625 (1981).

<sup>6</sup>Z. Iqbal and S. Veprek, J. Phys. C **15**, 377 (1982).

<sup>7</sup>I. H. Campbell and P. M. Fauchet, Solid State Commun. **58**, 739 (1986).

<sup>8</sup>H. D. Fuchs, M. Stutzmann, M. S. Brandt, M. Rosenbauer, J. Weber, A. Breitschwerdt, P. Deák, and M. Cardona, Phys. Rev. B **48**, 8172 (1993).

<sup>9</sup>Y. Kanzawa, S. Hayashi, and K. Yamamoto, J. Phys. Condens. Matter **8**, 4823 (1996).

<sup>10</sup>T. Takagahara, Phys. Rev. Lett. **71**, 3577 (1993).

<sup>11</sup>G. Mariotto, M. Montagna, G. Vilianni, E. Duval, S. Lefrant, E. Rzepka, and C. Mai, Europhys. Lett. **6**, 239 (1988).

<sup>12</sup>M. Fujii, S. Hayashi, and K. Yamamoto, Phys. Rev. B **44**, 6243 (1991).

<sup>13</sup>M. Fujii, T. Nagareda, S. Hayashi, and K. Yamamoto, J. Phys. Soc. Jpn. **61**, 754 (1992).

<sup>14</sup>N. N. Ovsyuk, E. B. Gorokhov, V. V. Grishchenko, and A. P. Shebanin, Pis'ma Zh. Éksp. Teor. Fiz. **47**, 248 (1988) JETP Lett. **48**, 678 (1988).

<sup>15</sup>B. Champagnon, B. Andrianasolo, A. Ramos, M. Gandais, M. Allais, and J. P. Benoit, J. Appl. Phys. **73**, 2775 (1993).

<sup>16</sup>A. Tanaka, S. Onari, and T. Arai, Phys. Rev. B **47**, 1237 (1993).

<sup>17</sup>M. Fujii, S. Hayashi, and K. Yamamoto, Jpn. J. Appl. Phys. **30**, 687 (1991).

<sup>18</sup>N. N. Ovsyuk and V. N. Novikov, Phys. Rev. B **53**, 3113 (1996).

<sup>19</sup>H. Lamb, Proc. London Math. Soc. **13**, 189 (1988).

<sup>20</sup>E. Duval, Phys. Rev. B **46**, 5795 (1992).

<sup>21</sup>M. Montagna and R. Dusi, Phys. Rev. B **52**, 10 080 (1995).

<sup>22</sup>A. Tamura, K. Higeta, and T. Ichinokawa, J. Phys. C **15**, 4975 (1982).

<sup>23</sup>E. Duval, A. Boukenter, and B. Champagnon, Phys. Rev. Lett. **56**, 2052 (1986).

<sup>24</sup>*American Institute of Physics Handbook*, 3rd ed. (McGraw-Hill, New York, 1972), pp. 3-102 and 3-105.